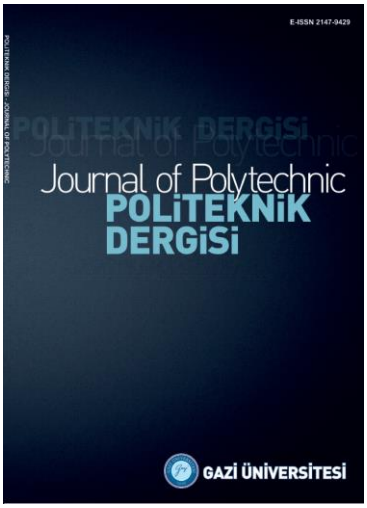

POLİTEKNİK DERGİSİ

JOURNAL of POLYTECHNIC

ISSN: 1302-0900 (PRINT), ISSN: 2147-9429 (ONLINE)
URL: http://dergipark.org.tr/politeknik

Energy absorption analysis of circular cross-section crashworthiness with dual gradient under axial and oblique loads

Dairesel kesitli ve dual gradyan çarpışma kutusunun eksenel ve eğik yükler altında enerji sönümleme analizi

Yazar(lar) (Author(s)): *Hakan Burçin ERDOĞUŞ[1]*

ORCID[1]: 0000-0002-2947-7510

To cite to this article: Erdogus H.B., "Energy absorption analysis of circular cross-section crashworthiness with dual gradient under axial and oblique loads", ***Journal of Polytechnic***, *(*): *, (*).

Bu makaleye şu şekilde atıfta bulunabilirsiniz: Erdoğuş H.B., "Energy absorption analysis of circular cross-section crashworthiness with dual gradient under axial and oblique loads", ***Politeknik Dergisi***, *(*): *, (*).

Erişim linki (To link to this article): http://dergipark.org.tr/politeknik/archive

DOI: 10.2339/politeknik.1335319

Energy Absorption Analysis of Circular Cross-Section Crashworthiness with Dual Gradient Under Axial and Oblique Loads

Highlights

- *Design variables for crashworthiness are used to determine performance parameters.*
- *The preparation of circular cross-sectional structures with inner panels as dual gradients increases the SEA value.*
- *In dual gradient structure designs, it is resistant to oblique loading and its folding shape can be controlled.*

Graphical Abstract

This study designed the structure with 8-panel elements with circular cross-sections as a dual gradient. The behavior of these designs under axial and oblique loading has been investigated in FE simulation. Theoretical and numerical analysis results were compared for SEA values.

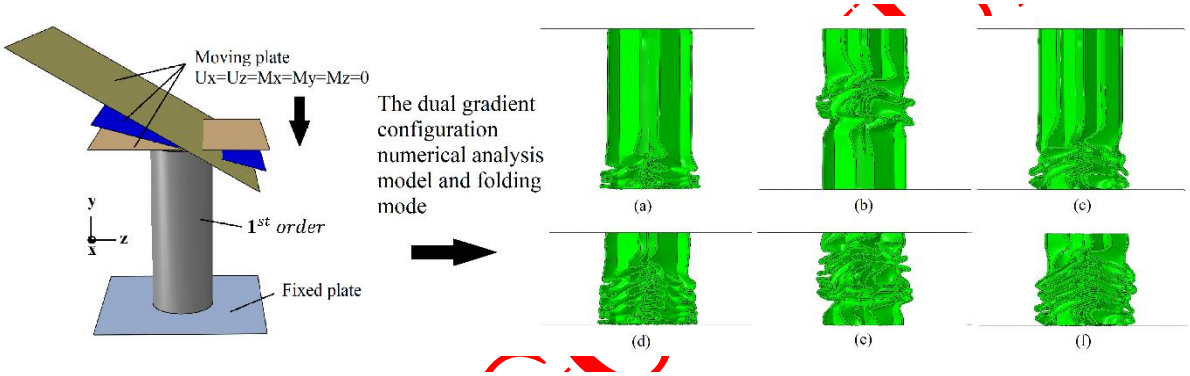

Figure. FE model assembly set up of three types structure and behaviors under axial loading.

Aim

The main purpose of this study is to present a new design by modeling crashworthiness structures as dual gradients.

Design & Methodology

For this study, the behavior of circular 8-panel structures under the impact of collision was investigated. The changes in performance parameters were interpreted by numerical and theoretical analysis methods.

Originality

Unlike the studies in the literature, the behavior of the dual gradient design under axial and oblique loading has been determined.

Findings

Compared to the 1^{st} order structure, it was determined that the 2^{nd} order configuration absorbs 12.95% more energy. In addition, it has been observed that while the 2^{nd} order design is advantageous to collapse under oblique loading conditions this design provide an unsufficient folding mode for plastic deformation.

Conclusion

The hierarchical distribution of panels at equal angles or the same geometric pattern with multicells is effective for achieving the best crashworthiness performance.

Declaration of Ethical Standards

The author(s) of this article declares that the materials and methods used in this study do not require ethical committee permission and/or legal-special permission.

Energy Absorption Analysis of Circular Cross-Section Crashworthiness with Dual Gradient Under Axial and Oblique Loads

Research Article

Hakan Burçin ERDOĞUŞ[1*]

[1]Izmir Kavram Vocational School, Department of Machinery and Metal Technologies, Izmir, Türkiye

(Received : 31.07.2023 ; Accepted : 30.11.2023 ; Early View : 20.08.2024)

ABSTRACT

The tube structures designed in the multicell pattern are used for crashworthiness in many areas. In this study, the crashworthiness was designed by dividing the inner area of the circular section geometry into equal slices by examining previous studies. In addition, this structure was prepared as a dual gradient in two different sizes along the length. Performance parameters were investigated by performing theoretical and numerical analyses. For multicell crashworthiness, which is considered a dual gradient, the folding style was insufficient in lobe formation. However, the specific energy absorption (SEA) and the crushing force efficiency (CFE) values of the two types of dual gradient structures behaved appropriately in absorbing kinetic energy. The dual gradient new design of crashworthiness provides resistance by preventing the bending of the structure under oblique loading. According to the results of the analysis, the mean SEA and CFE under loading at all angles for the 2 nd order dual gradient configuration was 12.88% and 1.61% higher than the 1st order design. However, with the preparation of circular section tubular structures using 8-panel elements, close values were obtained in the comparison of theoretical and numerical analysis under axial loading conditions

Keywords: Energy absorption, Crashworthiness, Dual gradient structures, Thin-walled structures.

Dairesel Kesitli ve Dual Gradyan Çarpışma Kutusunun Eksenel ve Eğik Yükler Altında Enerji Sönümleme Analizi

ÖZ

Çok hücreli desende tasarlanan tüp yapılar birçok alanda çarpmaya dayanıklı olarak kullanılmaktadır. Bu çalışmada daha önce yapılan çalışmalar incelenerek dairesel kesit geometrisinin iç alanı eşit dilimlere bölünerek çarpışma kutusu tasarlanmıştır. Ayrıca bu yapı, uzunluk boyunca iki farklı boyutta ikili gradyan olarak hazırlandı. Performans parametreleri teorik ve sayısal analizler yapılarak incelenmiştir. Çift gradyan olarak kabul edilen çok hücreli çarpışma dayanıklılığı açısından, lob oluşumunda katlanma stili yetersizdir. Bununla birlikte, iki tip çift gradyanlı yapının özgül enerji soğurma (SEA) ve çarpışma kuvveti verimliliği (CFE) değerleri, kinetik enerjinin sönümlenmesi konusunda uygun davranmıştır. Çarpışmaya dayanıklı yeni çift gradyanlı tasarım, eğik yükleme altında yapının bükülmesini önleyerek direnç sağlar. Analiz sonuçlarına göre, 2. derece çift gradyanlı konfigürasyonu için tüm açılardan yükleme altında ortalama SEA ve CFE, 1. derece tasarıma göre %12.95 ve %1.61 daha yüksek olmuştur. Ancak dairesel kesitli boru yapıların 8 panelli elemanlar kullanılarak hazırlanmasıyla eksenel yükleme koşulları altında teorik ve sayısal analizlerin karşılaştırılmasında birbirine yakın değerler elde edilmiştir.

Anahtar kelimeler: Enerji sönümleme, Çarpışma kutusu, Çift gradyanlı yapılar, İnce cidarlı yapılar.

1. INTRODUCTION

One of the important safety properties in vehicle design is the absorption of kinetic energy that occurs during a collision. Progressive folding of crashworthiness with plastic deformation prevents this energy from affecting the passenger and driver. In this context, cost reduction and efficiency are evaluated together for thin-walled outer frames such as square, triangular, or circular sections [1-3]. Hierarchical and multi-cell structures have gained importance in recent studies for energy absorber designs. Wang et al. [4] stated that the cross-panel configuration is suitable for providing the collapse mode as desired. Similarly, Nia and Parsapour [5] concluded that placing the panels in the corners of the square frame structure is higher than the mean crushing force (MCF) and the specific energy absorption (SEA). According to a study on the suitable design of circular-joint elements prepared to increase crashworthiness performance, the multiple cellular separations of the structure have increased the effect of performance parameters [6]. Fan et al. [7] concluded that the hierarchical order of structures and folding style are effective in MCF. Shen et al. [8] have shown that the structure divided into triple cell elements with rectangular outer frames provides optimal performance. Deng et al. [9] found that the crushing force efficiency (CFE) and energy absorption

* *Corresponding Author*
e-mail : hakan.erdogus@kavram.edu.tr

(EA) capacity of square tubes have improved to include multi-cell sections as dual gradients. In previous studies, experimental and numerical analysis was used for different configurations of multi-cells to enable the concertina mode of folding when the structures collapse in the circular outer frame. The shape and pattern of the inner panels play an important role in the CFE optimization of the circular outer frame of the structure. To reduce the fluctuation of the force-deformation curve, wall thicknesses, panel shape, and outer diameter are effective in the desired folding mode [10,11]. Tanbucu et al. [12] investigated a predictable theoretical model for MCF resulting from impact on a circular frame dividing into multiple cells. Considering the dynamic effects, it was stated that the coefficient should be between 1.4 and 1.6 in the theoretical calculations [13]. In the improvement of circular crashworthiness with multi-cell configuration, structures designed with bioinspired perspective have developed in decent years. The structures prepared with inspiration from plants and animals have much better energy absorption efficiency than other tubular designs [13-15]. Circular structures were inspired by plant stems divided into multiple sections with different shapes of panels, and studies were carried out on the most appropriate performance parameters [16-19]. San Ha et al. [20] determined that the wavelength of the force-deformation curve occurs differently from conventional tubular structures. The internal and external diameter of crashworthiness and the structural hierarchy of circular tubes play an important role in increasing SEA [21,22]. Greco et al. [23], inspired by bamboo, optimized the SEA value in crashworthiness in tube geometry with the number and shape of panels. Crashworthiness performance analysis is prepared not only under an axial collision but also under oblique loading. For circular frame crashworthiness, the size of the grooves on the outer frame has a significant effect on the oblique loading performance [24]. Fang et al. [25] performed oblique and axial loading of the structure in the square outer frame with multicell Accordingly, bending of the structure occurred by increasing the oblique loading angle. Huang et al. [26] determined that structures can be provided with an inner diameter close to the diameter of the outer frame to resist oblique forces acting at bigger angles. Qui et al. [27] found that progressive collapse is provided for small angles under oblique loads.

In this study, the performance of circular cross-sectional crashworthiness, which is divided into multi-cells at equal angles, was investigated. By considering the dual gradient design of these structures of equal weight, numerical analyses were performed at axial and oblique angles. However, a comparison of performance indicators of crashworthiness was calculated using the theoretical and numerical analysis method for SEA evaluation.

2. MATERIAL and METHOD

The hierarchical distribution of the multi-cell structures was mentioned in the crashworthiness efficiency of energy absorption [10,28]. To evaluate the crushing behavior of structures, the structure is aimed to reach a high load capacity with a small half-wavelength of force fluctuation. In this way, crashworthiness designs that are divided into multiple sections with panels are more advantageous than single-frame designs. This study used a circular tube divided into sections to provide controllable folding of the structure during deformation. The number of inner panels and corner shapes in multicell designs a critical role in energy absorption [29]. Here, three different configurations were designed for an 8-panel in the center and a 2-panel element in the corners, as shown in Figure 1.

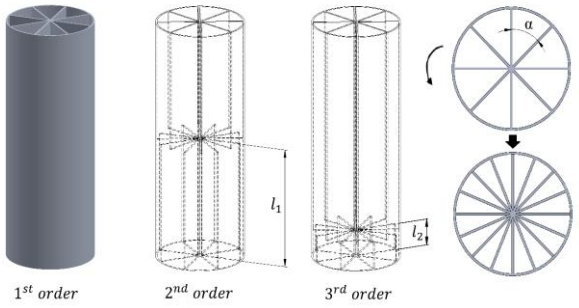

Figure 1. Three types of crashworthiness included dual configuration and top view.

According to the basic idea in the design, bending, and membrane energy theory were considered while performing the collapse mode. The mass of the three designs is the same at 0.391 kg, and the length and thickness are 200 mm and 1.41 mm, respectively. The panel angles are set to be $\alpha=\pi/8$ for uniform deformation, as shown in Figure 1. To provide controllable folding of the inner panels, the draft drawing was rotated counterclockwise $\pi/16$ to act as an internal trigger at half the length l_1=100 mm of the structure and a distance of l_2=20 mm.

3. NUMERICAL ANALYSIS

3.1. Performance Indicators of Crashworthiness

The kinetic energy generated by the impact of the moving plate is transformed into plastic deformation energy on the structures. In this process, the geometric characteristics of crashworthiness play an important role. The equations in the literature are used to calculate the performance indicators of structure. The main indicators calculated in performance measurements are, respectively: PCF (peak crushing force), MCF, SEA, EA, CFE, and energy absorption stability factor (EASF). The energy absorbed in the whole system during deformation:

$$EA(d) = \int_0^d F(x)dx \quad (1)$$

where d is the axial displacement and F is the axial crushing force. The maximum point on the force-displacement curve in numerical and experimental analyses is called PCF. The SEA is calculated by dividing EA by the mass of the structure [9]. Based on the force-deformation graph, the MCF is given as follows.

$$MCF(d) = \frac{EA(d)}{d} \quad (2)$$

CFE, which is the stability of the structure against the maximum impact force, can be explained as follows.

$$CFE = \frac{MCF}{PCF}\ x\ 100\% \quad (3)$$

Fan et al. [5] determined one of the accepted parameters for energy absorption performance in thin-walled structures as EASF. In this context, it can be written as follows concerning PCF and MCF ratio:

$$EASF = \frac{PCF}{MCF} \quad (4)$$

EASF increases crashworthiness with hierarchical patterns and inner panel geometries of multicell structures. The crashworthiness design is desired to have a low initial peak force at the crash. Although studies are focused on improving one or more parameters, they aim to reduce the waviness of forced displacement.

3.2 Description of Model and Validation

The multi-cell structures are designed with inner panels in various hierarchies with outer frames such as square and circular cross-sections. Wu et al.[30] investigated the structure of multicells with square cross-sectional crashworthiness in experimental and numerical studies. These structures were 200 mm in length and had various wall thicknesses. The boundary conditions of the plate and crashworthiness of the finite element (FE) assembly are shown in Figure 2(a). The moving and fixed plate was designed 100 x 100 mm² and steel used material properties, namely a density of 7800 kg/m³, Poisson's ratio of 0.3, and Young's modulus of 200 GPa. As seen in Figures 2(b) and 2(c), C1 and C4 are 75 x 75 mm² , design parameters which are given in Table 1 deformable 3D models designed in Solidworks were then imported into the simulation assembly.

Table 1. The parameters for FE model validation geometry [30].

	Outer thickness (mm)	Inner thickness (mm)
C1	2	-
C4	1.5	2

The structure's bottom surface and the outer surface of the fixed plate are constrained to each other. For this study, the design of which was verified, the FE model was established considering the material properties of AI6063-T5 as follows: density ρ=2700 kg/m³, Young modulus E=70 GPa, Poisson's ratio ν=0.3, yield stress σ_y=219 MPa and ultimate stress σ_u=250 MPa [9,13]. A static friction coefficient of 0.2 for surface-to-surface contact was defined as a quasi-static condition in the Abaqus/Explicit. The structures meshed the hexahedral reduced integrated element type (C3D8R). The wall thickness of the plates was 0.5 mm and were meshed shell element S3R.

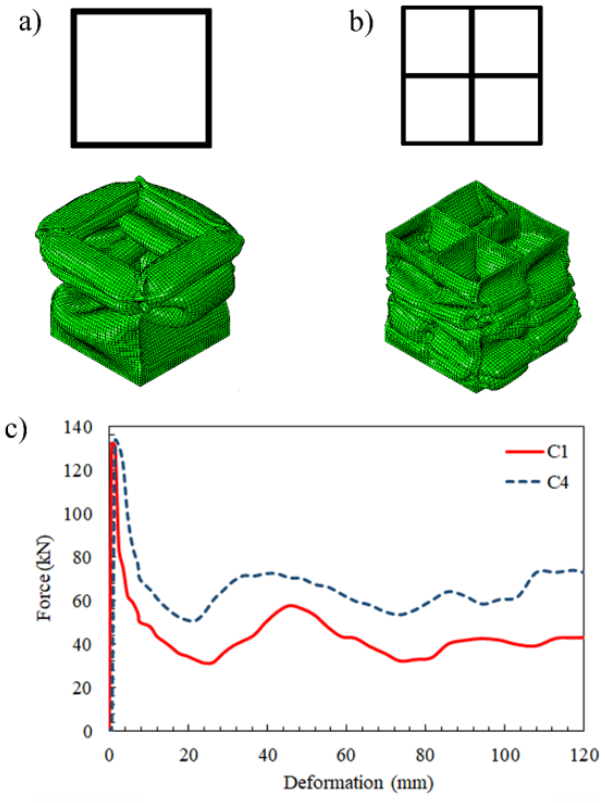

Figure 2. a) Square frame, b) Four cell design with inner panels, c) Force deformation curves of FE model validation.

Considering the deformation of structures by 120 mm, the moving plate velocity was determined at 10 m/s [16,26,30,33]. According to the quasi-static analysis solution, the ratio of kinetic energy to internal energy is below 5% for the validation of FE. The force-deformation curve of C1 and C4, which were designed in the same mass but with different wall thicknesses, was carried out as shown in Figure 2(a). The cross-sectional areas of the C1 and C4 structures were equal; thus, the PCF was 132.21 kN and 133.77 kN, respectively. Until the sustained deformation to 120 mm, C4 collapse modes were more uniform than C1, as illustrated in Figure 2(b)-2(c).

In the impact simulation applied to the C1* and C4* structures for FE model verification, C1 and C4 were calculated by the force-deformation curve and Eq(1),(2), and (3). As given in Table 2, according to the referenced results, model validation was approved since the mean error in the simulation model was below 5%.

3.3 FE Model Assembly with Axial and Oblique Loads

In this study, the crushing performance of the new design was investigated in the FE model with axial and oblique loads. The FE simulation model was set up as shown in Figure 3. The moving plate was constrained to all degrees of freedom except y-direction and the fixed plate was encastered at the bottom of the crashworthiness.

Table 2. FE model verification of crashworthiness indicators for the reference study.

	PCF(kN)	MCF(kN)	SEA(kJ/kg)	EA(kJ)	CFE(%)
C1* [30]	132.21	44.75	13.7	5.37	33.85
C1	131.37	42.66	12.64	5.11	32.5
C4* [30]	145.42	69.16	20.48	8.29	47.6
C4	133.77	67.06	20.54	8.05	50.15
Absolute mean error (%)	-4.32	-3.83	-1.26	-3.86	0.55

It was prepared in different sizes to provide 120 mm crushing of the moving plate at three different angles (0°-15°-30°) of the structures. These plates were displaced 5 mm above the structure. In the simulation of deformation for crushing performance, while one moving plate was applied for 120 mm deformation under axial and oblique loads on the structures, other moving plates were inactivated in the y-direction

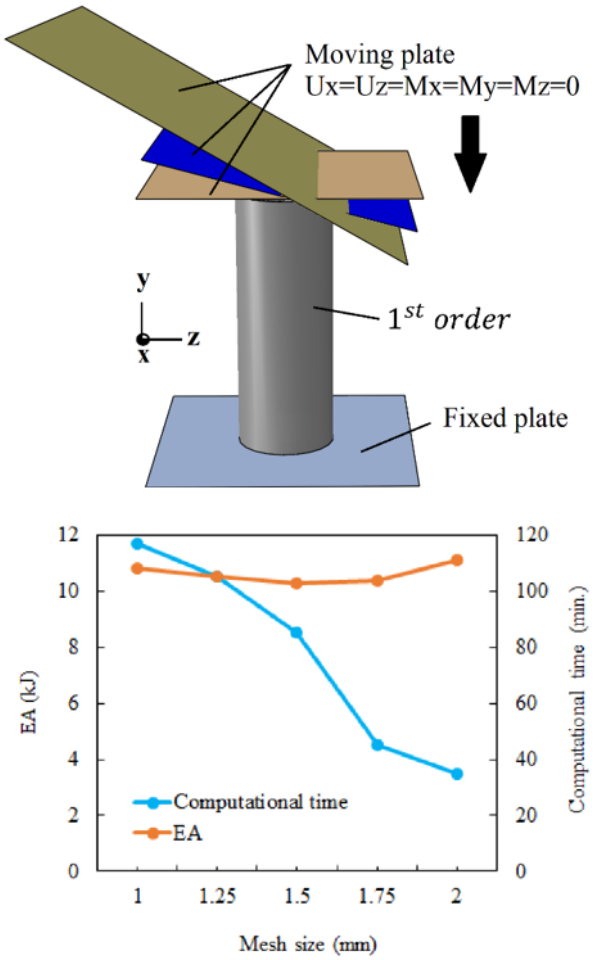

Figure 3. The FE model illustration and mesh convergence analysis.

For the mesh size convergence of the numerical analysis, the 1^{st}order structure was gridded into 1 mm, 1.25 mm, 1.5 mm, 1.75 mm, and 2 mm. As seen in Figure 3, when the computational time increased, the EA curve remained at a plateau. Here, all of the structures in analysis for precise results used the mesh type 8-noded linear brick element (C3D8R), and the mesh size is set as 1x1 mm² [24].

3.4 Numerical Results

3.4.1. Crushing behavior under axial loads

In the circular sectional crashworthiness, the force-deformation curves for the different configurations related to the position of the inner panels were obtained as shown in Figure 4.

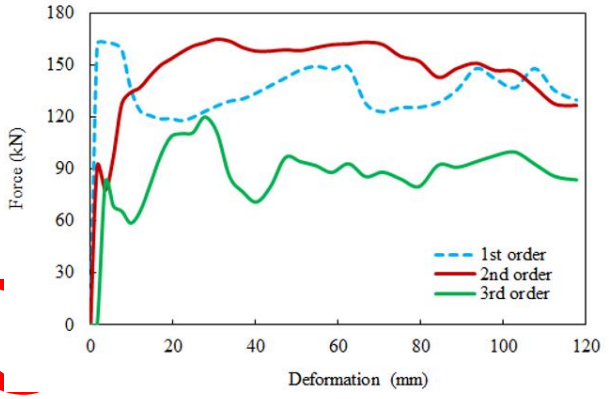

Figure 4. The force-deformation curves of circular tubes for axial loading.

Here, while the force is impacted by the moving plate on the structure, the progressive collapse of the structure is absorbed by the deformation. Generally, the structure geometry independent of the cross-section can change in crashworthiness performance, as well as the wavelength can increase after the initial impact stage [16]. To utilize as a trigger of the configurations (2^{nd} and 3^{rd}order) with the same panel distribution was placed in the structure by rotating $\pi/8$. The force-deformation curve of fluctuation in these two designs showed a small wavelength behavior throughout the deformation. Unlike similar studies, the force-deformation curve remained stable throughout deformation without initially high PCF for 3^{rd}order configuration. In the 1^{st}order structure, the PCF increased during continued deformation causing increased MCF. In fact, for ensuring passenger and driver safety, it is considered a positive impact that the force does not increase in the case of the densification stage. When the structure is resistant to high impacts under the effect of crushing, controllable plastic deformation provides a plateau force-deformation curve. As illustrated in the cross-section of crashworthiness configurations in Figures 5(a) and 5(d), the folding shape of the 1^{st}order structure was deformed by the moving plate displacement of 60 mm and 120 mm. It is demonstrated in cross-sections of 2^{nd}order structure in

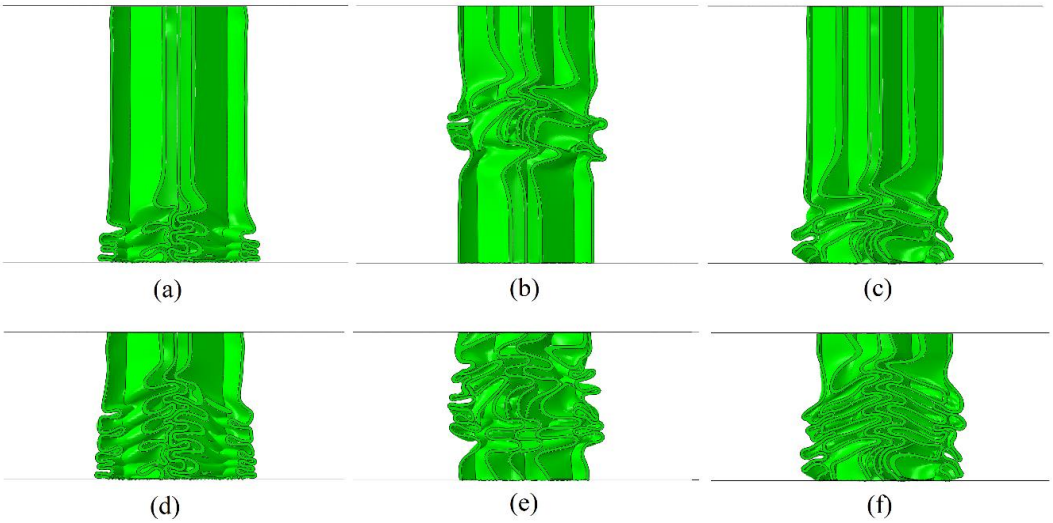

Figure 5. The axial deformation of structures from 60 mm to 120 mm (a)-(d) 1^{st}order, (b)-(e) 2^{nd}order, (c)-(f) 3^{rd}order.

Figures 5(b) and 5(e) that the 8-panel basic geometry is rotated π/8 and placed half of the structure, ensuring trigger effect. As given in Figure 5, the inner panels decreased the deformation during the impact. The progressive deformation of 2^{nd}order configuration started at the end of the first half and then continued in the other half of the structure. While the collapse of structures in the conventional 1^{st}order started from the base, in the other two configurations, the collapse mode has generated maneuverability of folding at the distances of panels. In the 3^{rd}order configuration ensured the progressive folding of the whole structure as seen in Figures 5(c) and 5(f). The panels positioned inside of structures ensured a concertina mode of deformation during the collision. In this way, the PCF is prevented from rising during deformation. However, it has been stated that the energy absorption ability is increased with the rib forms found in half of the square tube structure [34]. As a result of the numerical analysis, the MCF calculated for axial loads were 131.34 kN, 155.80 kN, and 87.14 kN, respectively. In addition, MCF in the 3^{rd}order structure decreased by approximately 64 % compared to the other two configurations. It is noted that the distance of the rips or panels placed inside the structures from the impact surface is more important to reduce the deformation rate and increase energy absorption.

3.4.2. Crushing behavior under oblique loads

In general, the reality of vehicle crashes, is that crashworthiness which are placed in bumpers absorb deformation at different angles. Therefore, oblique loads are also considered in numerical analysis for crashworthiness designs. In this study, the deformation caused by the 15° and 30° inclined plates was investigated by crushing three different configurations with a moving plate of 10 m/s. The inclined moving plate deformed structures on the displacement of y-direction 120 mm as illustrated in Figure 6 and Figure 7.

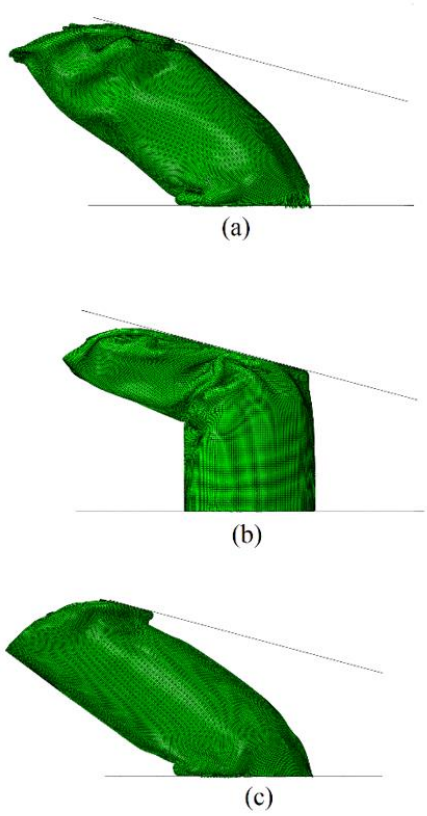

Figure 6. The 120-mm deformation of structures at 15° under oblique loads (a) 1^{st}order, (b) 2^{nd}order, (c) 3^{rd}order.

It can be seen from Figure 6(a) that when the collision behavior at different angles is applied, the folding mode is stable in the 1^{st}order design at a 15° angle. Meanwhile, under 30° loading, the structure is bending as shown in Figure 7(d). On the other hand, while the $2^{nd}$and

3^{rd}order structures are considered to have a dual gradient, they collapse under force. As can be seen in Figures 6(b) and 6(c), the structures of the dual gradient collapsed against oblique loads. According to the $2^{nd}$and 3^{rd}order structures, the numerical analysis indicated a small folding mode with lower plastic deformation than the 1^{st}order on the top of the structures under loading at 30° angles, as demonstrated in Figure 7(e)-6(f). Also, the $2^{nd}$and 3^{rd}order structures with inner panels have occured small plastic deformation and higher resistance than 1^{st}order to collapse under oblique load. The numerical results indicated that MCF, one of the important parameters in the impact of structures, occurred at the highest value with 68 kN for the 2^{nd} order. Therefore, the energy absorption capacity of the structure with such internal panels increases under 15° loading conditions.

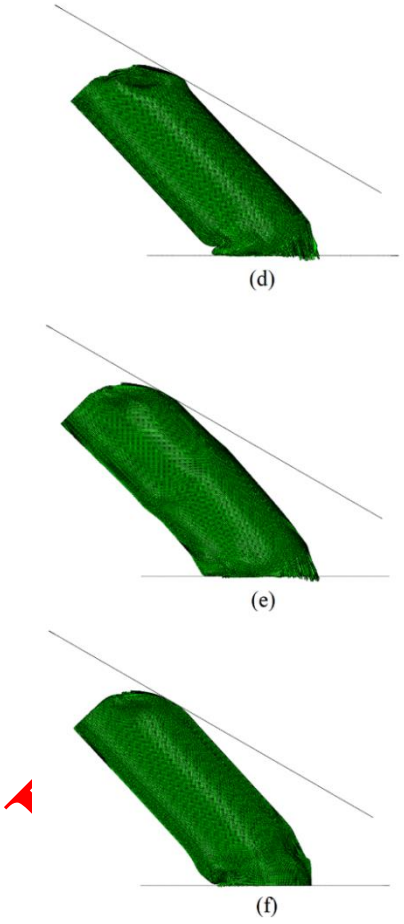

Figure 7. The 120-mm deformation of structures at 30° under oblique loads (d) 1^{st}order, (e) 2^{nd}order, (f) 3^{rd} order.

In addition to the fact that axial forces are always decisive during a collision in vehicles, oblique loading of structures also has a confirmatory effect in terms of design improvement. Hence, the deformation caused by the 15° and 30° moving plates is mentioned as the performance merit of the 2^{nd}order crashworthiness under the impact of oblique loading.

4. THEORETICAL ANALYSIS

To examine the effects of crashworthiness design parameters, a simplified super folding element (SSFE) is used, which helps to perform theoretical analysis [9,16]. In the basic equation, as seen in Eq (5) discussed to determine EA and SEA, it is assumed that concertina mode occurs with full folding of the panel elements [9,13,16]. Subsequently, the deformation at a certain distance transforms the kinetic energy of crushing into bending ($E_{bending}$) and membrane energy ($E_{membrane}$).

$$MCF.2Hk = E_{bending} + E_{membrane} \quad (5)$$

Where 2H is the wavelength of panel deformation for each fold, and k is the effective crushing distance coefficient depending on wavelength. The real crushing deformation occurs due to the incomplete folding of panels. This study used a value of 0.71 for the k coefficient [9]. The bending energy can be calculated when the three panels acting like plastic hinges fold completely flat as follows.

$$E_{bending} = \sum_{i=1}^{3} M_b \, \emptyset_i \, L_t \quad (6)$$

Where $\emptyset_i$ is the rotation angle at each plastic hinge, L_t is the total perimeter length of the structure relative to the cross-sectional area, and the fully plastic bending moment is determined as $M_b = \sigma_0 t^2/4$ The flow stress is calculated as $\sigma_0 = \sqrt{\frac{\sigma_y \sigma_u}{1+n}}$ where σ_y and σ_u are the yield strength and ultimate strength, respectively, n is the strain hardening exponent and is set to be 0.06 for the AI-6063-T5 [9] and t is the thickness of the structure. The rotation angles at the three hinges are π/2, π/2, and π respectively based on the complete folding of the panels. Thus, the bending energy can be explained as.

$$E_{bending} = 2\pi M_b L_t \quad (7)$$

The energy dissipation caused by the membrane deformation of the 8-panel element in the center of the 1^{st} order tube structure and the 2-panel elements attached to the outer frame is marked in Figure 8.

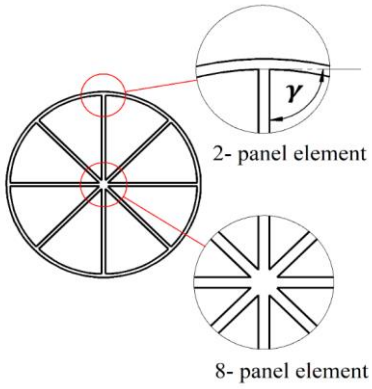

Figure 8. The schematic visualization of basic elements with inner panels.

The two symmetrical criss-cross elements are combined for an 8-panel element and the membrane energy is calculated as [9].

$$E_{8-panel} = 2\,E_{criss-cross} = 32\,M_b\frac{H^2}{t} \quad (8)$$

To consider the γ angle is π/2, the membrane energy of the 2-panel elements is as follows [16].

$$E_{2-panel} = \frac{4M_bH^2}{t}\left(tan\frac{\gamma}{2} + 2sin\gamma\right) = \frac{12M_bH^2}{t} \quad (9)$$

The total membrane energy in the structure consists of the sum of the membrane energy of all elements as defined.

$$E_{membrane} = n_8\frac{32M_bH^2}{t} + n_2\frac{12M_bH^2}{t} \quad (10)$$

For calculating EA and SEA at the 1^{st}order of tube structure, Eq. (5) is written as follows.

$$MCF\,.2Hk = 2\pi M_bL_t + n_8\frac{32M_bH^2}{t} + n_2\frac{12M_bH^2}{t} \quad (11)$$

The stationary condition is used to determine the half-wavelength as follows.

$$\frac{\partial MCF}{\partial H} = 0 \quad (12)$$

Substituting Eq. (12) into Eq. (11), the theoretical equation of MCF can be described as.

$$MCF = \frac{1}{2k}\sigma_0 t\sqrt{(16\,n_8 + 6\,n_2)\pi L_t t} \quad (13)$$

The dynamic enhancing coefficient $k_d$was considered for 1^{st} , $2^{nd}$and 3^{rd}order 1.1,1.05 and 1, respectively, with respect to the axial deformation of the crashworthiness at the crushing distance under quasi-static conditions [13]. Combining Eq. (1), Eq.(2), and Eq(13), EA and SEA are calculated as follows.

$$EA = \frac{\sigma_0 t d k_d}{2k}\sqrt{(16\,n_8 + 6\,n_2)\pi L_t t} \quad (14)$$

$$SEA = \frac{k_d\sigma_0 d}{2k\rho L}\sqrt{(16\,n_8 + 6\,n_2)\pi t L_t} \quad (15)$$

5. COMPARISON of RESULTS and VALIDATION

5.1. Force-deformation Curves Under Oblique Loads

In this section, the energy absorption performance of the three designs is investigated under axial and oblique loading. As can be seen in Figure 9(a), during the force-deformation curve plotting in the simulation, energy absorption was recorded to force fluctuation under loading at 15° on the 1^{st}order structure. While the oblique load is impacted on the dual gradient of the two structures (2^{nd} and 3^{rd} order), the tendency of the force-deformation curve is similar as shown in Figure 9(a).

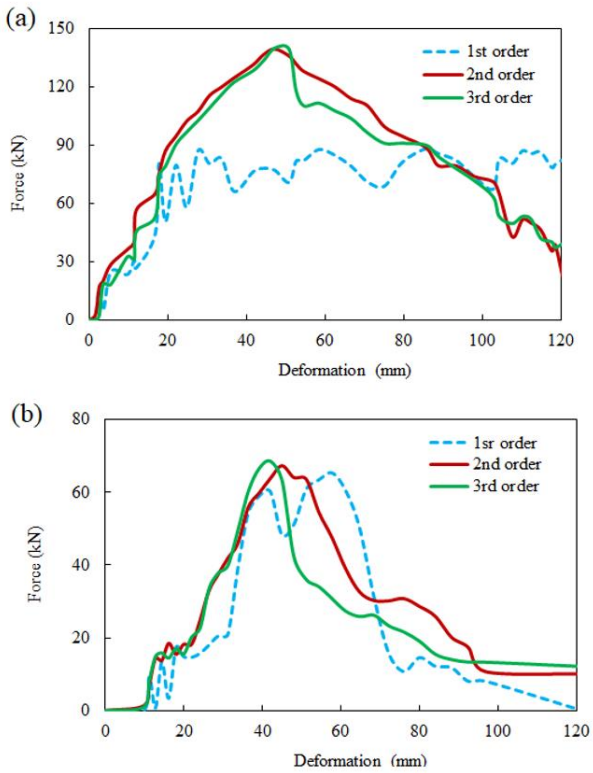

Figure 9. Force deformation curves of structures under a loading angles (a) 15° and (b) 30°.

The PCF values of the $2^{nd}$and 3^{rd}order designs were determined as 139.68 kN and 140.15 kN, respectively at 15° loading. Here, all the designs showed similar behavior under a 30° loading angle. San Ha et al.[13] demonstrated that the force-deformation curves occurred similarly to bioinspired circular structures under 30° oblique loading.

However, the 2^{nd}order structure provided more reaction force between 40 and 60 mm. The reaction forces decrease when oblique loading is applied on the distal center, as shown in Figure 9(b). The reaction forces of $2^{nd}$and 3^{rd}order structures have reduced depending on the bending of structures instead of deformation. In the simulation of 2^{nd}order configuration, there were two points of PCF, 139.68 kN, and 67.34 kN, at 15° and 30°, respectively. On the other hand, 140.15 kN and 68.58 kN peak forces have been obtained in the 3^{rd} order. Additionally, the force-deformation curve started to decrease at the same tangency in all configurations from the PCF point to the completed deformation. According to the force-deformation curves, the structure was enabled to absorb kinetic energy with plastic deformation energy up to 40 mm deformation. Afterward, the reaction forces decreased between 40-60 mm as the structure began to collapse under the bending effect with inclined loads. These studies showed that the force-deformation curves were similar fluctuation for multi-cell structures with circular cross-sections [13]. Overall, with the increase of SEA, the MCF increases in impact conditions. At the same time, driver and passenger safety can be

protected by ensuring stability by a small wavelength of force-deformation curve and ensuring minimum PCF into the deformation process.

5.2. Energy Absorption

The energy absorption increased from the top of the structures to the deformation of 120 mm, as shown in Figure 10. In axial loading, the 2^{nd} order configuration absorbed 18.6 % more energy than the 1^{st}order design, as given in Figure 10(a). To improve the energy absorption of structures with inner panels which are placed at a distance of 20 mm from the base of the structure was performed the 3^{rd}order and 1^{st}order. According to the comparison of the EA performances of these two structures mentioned, it has been observed that the 3^{rd}order structure absorbs 50 % more energy than the 1^{st}order. Most researchers concluded that the CFE and EASF were important for improving the design in measuring crashworthiness performance criteria. Fan et al. [7] determined that the most appropriate energy absorption can be provided when the EASF value is close to "1".

Compared to EA, CFE and EASF of the structures, the 2^{nd}order configuration ensured the advantages of axial crushing. Despite this, PCF and MCF increased at the same tangency as a bioinspired design [16] correlated with plastic deformation and folding shape of the

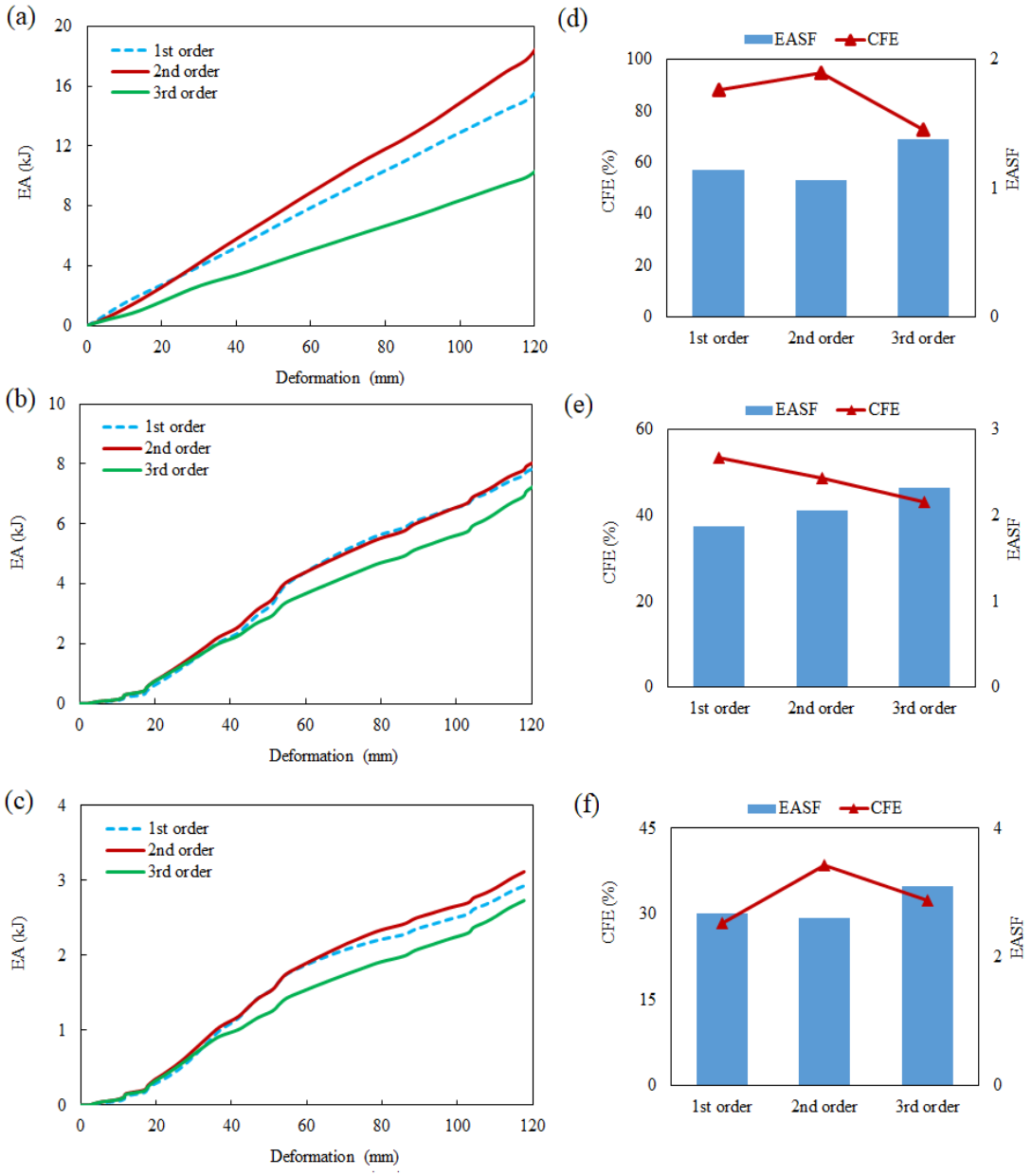

Figure 10. Comparison of EA, EASF and CFE under loading angles: (a)-(d) axial ,(b)-(e) 15°,(c)-(f) 30°.

structures under axial loads. The CFE increases as the 2^{nd} and 3^{rd} order structures as shown in Figure 10(d) and is attributed to high resistance to the crushing force.

The 1^{st} order design provided approximately 9.7% and 23.9% higher CFE than the other two configurations for an oblique load angle of 15°, as seen in Figure 10(b). In addition, as demonstrated in Figure 10(e), the EASF value of 1^{st} order was close to 1, giving a suitable result compared to the dual gradient designs. The EA was determined to be 8.16 kJ with the outer frame and inner panels partially folded by the inclined plate for the 2^{nd} order structure. Also, the EA of the 2^{nd} order was 3.9 % and 12.5 % higher than the 1^{st} and 3^{rd} order structures, respectively. The reason for this is that the energy absorption was reduced in dual gradient designs as it becomes difficult to fold the structure walls. As seen in Figure 10(c), a similar EA-deformation curve was plotted in all three structures under loading the inclined plate acting at a 30° angle. Here, the 30° oblique loading applied on the structures increased the EASF with the increase in the differences between PCF and MCF values. Therefore, it was determined that the 2^{nd} order structure had suitable behavior compared to other structures with a low EASF ratio of 2.61 and CFE was 18.35% higher than 1^{st} order, as given in Figure 10(f).

5.3. Comparisons of SEA in all Configurations of Crashworthiness

In this section, to compare the SEA for three crashworthiness was investigated on the 120-mm deformation. Therefore, theoretical and numerical analysis methods were used for the variation of SEA concerning deformation, as seen in Figure 10. In crashworthiness analysis, the most known principle criterion, the SEA which is independent of the geometric shape from the performance criteria but a characteristic feature of the energy absorbed by the mass, plays a significant role in selecting the optimal design. Focusing on the numerical analysis for SEA, the 2^{nd} order structure was higher than the other two designs under all load applications.

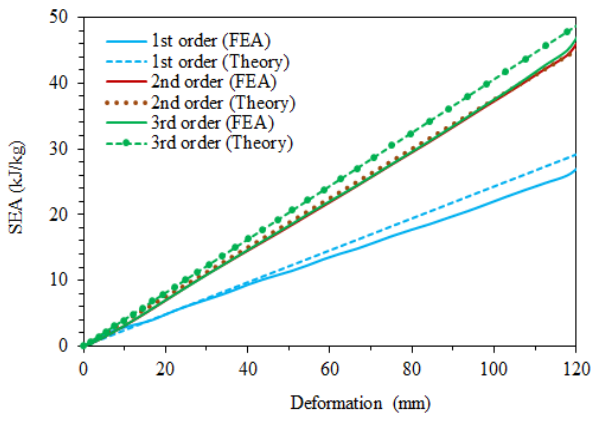

Figure 11. Theoretical and numerical analysis results of SEA for deformation depth.

The SEA values were different compared to EA values for three structures prepared with equal mass and different configurations. Regarding the oblique loads, the SEA was calculated as 20.08 kj/kg, 20.87 kj/kg and 18.54 kj/kg, respectively under 15° inclined loads. Similarly, it was determined as 7.49 kj/kg, 7.95 kj/kg and 6.80 kj/kg under 15° loading conditions. The EA increases during deformation due to the effect of angular impact, SEA also increases.

As seen in Figure 11, the absolute mean errors for SEA calculated with Eq.(15) and determined by numerical results are 7.7%, -2.6%, and 3.4%, respectively. In previous studies, the dynamic coefficient ranged from 1.05 to 1.6 in theoretical calculations [13,31]. Here, the dynamic coefficient is selected as 1.1, 1.05, and 1 for the configurations of multicell structure, which is considered the basic design.

5.4. Selecting the Optimal Configuration

The basic criteria for evaluating the performance of the structures prepared with dual configuration are presented in Table 3. It is noted that the mean values of main performance parameters were involved under axial and oblique loading. The CFE value of the 2^{nd} order design ensured above 1.61% merit compared to the 1^{st} order. On the other hand, 2^{nd} order structure provided 12.95% more energy absorption than 1^{st} order. The structure included half of the length configuration is sufficient to increase the energy absorption capacity of the structures [32].

In the theoretical and numerical analysis evaluation, it means that with the increase in CFE, the MCF value increases at a similar ratio. When EA and SEA are investigated together, the 2^{nd} order design becomes preferable as it reaches the densification stage as a plateau without fluctuation in the force-deformation curve. A close result was obtained with the SEA and EA values determined by Altın [33], with its 8-panel circular design. According to the square outer frame dual gradient structural design model, it was observed that the SEA efficiency was improved by maintaining equal mass [9].

6. CONCLUSION

In this study, the performance parameters of an 8-panel structure with a circular cross-section were prepared as two different dual gradients. For this, model validation was carried out using a crashworthiness design with a square section with four sections. Theoretical equations of the criteria were determined for performance indicators in crashworthiness designs based on a circular cross-section design. The following results can be summarized:

1. The energy absorption ability of circular cross-section structures was increased with multi cells and the number of panels in the crashworthiness wall. The hierarchical distribution of panels at equal angles or the same geometric pattern with multicells is effective for achieving the best performance of crashworthiness.

Table 3. The mean values of the performance criteria were determined under axial and oblique loads for numerical analysis.

	EA (kj)	MCF (kN)	SEA (kj/kg)	CFE (%)	EASF
1^{st} order	8.80	73.73	22.51	59.60	2.15
2^{nd} order	9.94	83.24	25.41	60.56	1.9
3^{rd} order	6.76	56.58	17.29	49.36	2.26

2. As in many studies, the folding style is similar in circular tubes under axial loading. It was determined that the dual gradient structures designed for this study showed the same behavior under axial loading. The 2^{nd}order structure means SEA value was determined at 25.41 kj/kg in the numerical analysis at all angles (0°-15°-30°).

3. Although the mean CFE increased in dual gradient designs with half distances of length, the force-deformation curve remained stable as a plateau. Similar behavior was also observed in bioinspired structures. In the analysis of crashworthiness structures, a fluctuation of the force-deformation curve with a high PCF value is expected due to the impact of the collision. Principally, manufacturability and experimental studies are required for the performance of crashworthiness structures designed as dual gradients in future studies.

DECLARATION of ETHICAL STANDARDS

The author(s) of this article declare that the materials and methods used in this study do not require ethical committee permission and/or legal-special permission.

AUTHORS' CONTRIBUTIONS

Hakan Burçin ERDOĞUŞ: Performed the simulations, made evaluations, and wrote the whole manuscript.

CONFLICTS of INTEREST

No conflict of interest was declared by the authors.

REFERENCES

[1] Nia A. A. and Parsapour M., "Comparative analysis of energy absorption capacity of simple and multi-cell thin-walled tubes with triangular, square, hexagonal, and octagonal sections", ***Thin-Walled Structures***, 74: 155-165, (2014).

[2] Altın M., ve Yücesu H. S., "Farklı geometrik yapılardaki çarpışma kutularının içerisine yerleştirilen alüminyum köpük malzemenin enerji sönümleme kapasitesi üzerine etkisinin incelenmesi", ***Politeknik Dergisi***, 22(1): 141-148, (2019).

[3] Yıldız B., "Aritmetik Optimizasyon Algoritması Kullanarak Taşıt Elemanlarının Çarpışma Performansının Eniyilemesi", ***Politeknik Dergisi***, 26(3): 1277-1283, (2023).

[4] Wang Z., Liu J., Yao S., "On folding mechanics of multi-cell thin-walled square tubes", ***Composites Part B: Engineering***, 132: 17-27, (2018).

[5] Nia A. A. and Parsapour M., "An investigation on the energy absorption characteristics of multi-cell square tubes", ***Thin-Walled Structures***, 68: 26-34, (2013).

[6] Wu Y., Fang J., He Y., Li W., "Crashworthiness of hierarchical circular-joint quadrangular honeycombs", ***Thin-Walled Structures***, 133: 180-191, (2018).

[7] Fan H., Luo Y., Yang F., Li W., "Approaching perfect energy absorption through the structural hierarchy", ***International Journal of Engineering Science***, 130: 12-32, (2018).

[8] Shen W., Gu X., Jiang P., Hu J., Lv X., Qian L., "Crushing analysis and multiobjective optimization design for rectangular unequal triple-cell tubes subjected to axial loading", ***Thin-Walled Structures***, 117: 190-198, (2017).

[9] Deng X., Lu Q., Liu F., Huang, J., "Energy absorption comparison of conventional and dual gradient hierarchical multicellular tubes under axial impact", ***Journal of the Brazilian Society of Mechanical Sciences and Engineering***, 45(3): 182, (2023).

[10] Acar E., Altin M. U. R. A. T., Güler M. A., "Evaluation of various multi-cell design concepts for crashworthiness design of thin-walled aluminum tubes", ***Thin-Walled Structures***, 142: 227-235, (2019).

[11] Ahmed N., Xue P., Kamran M., Zafar N., Mustafa, A., Zahran, M. S., "Investigation of the energy absorption characteristics of metallic tubes with curvy stiffeners under dynamic axial crushing", ***Latin American Journal of Solids and Structures,*** 14: 1293-1313, (2017).

[12] Tabacu S., "Axial crushing of circular structures with rectangular multi-cell insert", ***Thin-Walled Structures,*** 95: 297-309, (2015).

[13] San Ha N., Pham T. M., Chen W., Hao H., "Energy absorption characteristics of bio-inspired hierarchical multi-cell bi-tubular tubes", ***International Journal of Mechanical Sciences***, 251:108260, (2023).

[14] San Ha N. and Lu G.,"A review of recent research on bio-inspired structures and materials for energy absorption applications", ***Composites Part B: Engineering***, 181: 107496, (2020).

[15] Qin S., Deng X., Liu X., "Crashworthiness analysis of bioinspired hierarchical gradient multicell tubes under axial impact", ***Thin-Walled Structures***, 179: 109591, (2022).

[16] Gong C., Hu Y., Bai Z., "Crashworthiness analysis and optimization of lotus-inspired bionic multi-cell circular tubes", ***Mechanics of Advanced Materials and Structures,*** 1-19, (2022).

[17] Gong C., Bai Z., Lv J., Zhang L., "Crashworthiness analysis of bionic thin-walled tubes inspired by the evolution laws of plant stems", ***Thin-Walled Structures***, 157: 107081, (2020).

[18] Xiao Y., Yin H., Fang H., Wen G., "Crashworthiness design of horsetail-bionic thin-walled structures under axial dynamic loading", ***International Journal of Mechanics and Materials in Design,*** 12: 563-576, (2016).

[19] Cheng X., Bai Z., Zhu F., Chou,C. C., Jiang B., Xu S., "An optimized bio-inspired thin-walled structure with controllable crashworthiness based on magnetorheological fluid", ***Mechanics of Advanced Materials and Structures***, 1-16, (2022).

[20] San Ha, N., Lu G., Xiang X., "High energy absorption efficiency of thin-walled conical corrugation tubes mimicking coconut tree configuration", ***International Journal of Mechanical Sciences,*** 148: 409-421, (2018).

[21] Zou M., Xu S., Wei C., Wang H., Liu Z., "A bionic method for the crashworthiness design of thin-walled structures inspired by bamboo", ***Thin-Walled Structures***, 101: 222-230, (2016).

[22] Zhang W., Yin S., Yu T. X., Xu J., "Crushing resistance and energy absorption of pomelo peel inspired hierarchical honeycomb", ***International Journal of Impact Engineering,*** 125: 163-172, (2019).

[23] Greco L., Buccino F., Xu Z., Vergani L., Berto F., Guagliano M., Bagherifard S., "Design and analysis of energy absorbent bioinspired lattice structures", ***Journal of Bionic Engineering***, 1-17, (2023).

[24] Tian K., Zhang Y., Yang F., Zhao Q., Fan H., "Enhancing energy absorption of circular tubes under oblique loads through introducing grooves of non-uniform depths", ***International Journal of Mechanical Sciences,*** 166: 105239, (2020).

[25] Fang J., Gao Y., Sun G., Qiu N., Li Q., "On design of multi-cell tubes under axial and oblique impact loads", ***Thin-Walled Structures***, 95: 115-126, (2015).

[26] Huang H., Xu S., "Crashworthiness analysis and bionic design of multi-cell tubes under axial and oblique impact loads", ***Thin-Walled Structures***, 144: 106333, (2019).

[27] Qiu N., Gao Y., Fang J., Feng Z., Sun G., Li Q., "Crashworthiness analysis and design of multi-cell hexagonal columns under multiple loading cases", ***Finite Elements in Analysis and Design***, 104: 89-101, (2015).

[28] Tsang H. H., Raza S., "Impact energy absorption of bio-inspired tubular sections with structural hierarchy", ***Composite Structures,*** 195: 199-210, (2018).

[29] Xu S., Li W., Li L., Li T., Ma C., "Crashworthiness design and multi-objective optimization for bio-inspired hierarchical thin-walled structures", ***Computer Modeling in Engineering & Sciences,*** 131(2): 929-947, (2022).

[30] Wu S., Zheng G., Sun G., Liu Q., Li G., Li Q., "On design of multi-cell thin-wall structures for crashworthiness", ***International Journal of Impact Engineering,*** 88: 102-117, (2016).

[31] Zhang L., Bai Z., Bai F., "Crashworthiness design for bio-inspired multi-cell tubes with quadrilateral, hexagonal and octagonal sections", ***Thin-Walled Structures,*** 122: 42-51, (2018).

[32] Zhang J., Zheng D., Lu B., Zhang T., "Energy absorption performance of hybrid cross-section tubes under oblique loads", ***Thin-Walled Structures***, 159:107133, (2021).

[33] Altın M., "Çarpışma kutularının üzerine açılan oyukların çarpışma performansı üzerine etkisinin incelenmesi", ***Politeknik Dergisi***, 22(1): 135-139, (2019).